III-1 A NON-RECIPROCAL FERRITE HYBRID

M. Omori

Bell Telephone Laboratories, Inc.

The paper reports a new type of ferrite device, a single junction, nonreciprocal hybrid. There are four symmetrical ports exiting from the junction any one of which may be considered the input. The input energy splits into the two side ports with the signals 90° out of phase from each other. The opposite port is isolated from the input. The phase shift between any two ports is nonreciprocal. Further, with shorts placed properly on the side ports, the device becomes a gyrator.

First, the realizability of the device is shown by satisfying the unitary condition of the idealized scattering matrix. Then the operation of the hybrid is explained by the combination of two degenerate modes of the junction. Finally, the performance of an actual L-band model is shown.

The ideal scattering matrix of a symmetrical hybrid junction may be expressed as follows:

$$[S] = \begin{bmatrix} 0 & 0 & B & C \\ 0 & 0 & C & B \\ C & B & 0 & 0 \\ B & C & 0 & 0 \end{bmatrix}$$

The reciprocity relations, $S_{mn} = S_{nm}$ do not hold for this case, since the junction is nonreciprocal. Assuming a lossless junction, the conservation of energy or unitary condition can be satisfied by letting

$$B = \frac{1}{2}(1 + j)$$

$$C = \frac{1}{2}(1 - j)$$

or

$$[S] = \frac{1}{\sqrt{2}} \begin{bmatrix} 0 & 0 & e^{j\pi/4} & e^{-j\pi/4} \\ 0 & 0 & e^{-j\pi/4} & e^{j\pi/4} \\ e^{-j\pi/4} & e^{j\pi/4} & 0 & 0 \\ e^{j\pi/4} & e^{-j\pi/4} & 0 & 0 \end{bmatrix} \tag{1}$$

Therefore, a hybrid which is symmetrical for all four ports is physically realizable by utilizing nonreciprocal elements.

The structure which gives the hybrid performance is shown in Figure 1. The shorting posts at the top and bottom of the center conductor are introduced to bring the frequency of the TM_{010} mode near the TM_{110} mode, which is less affected by the posts. When the TM_{110} mode splits into two nondegenerate modes because of the tensor permeability of the ferrite rings, the lower mode, TM_{110}, can become degenerate with the lowest mode, TM_{010}. With this degeneracy condition satisfied and the loaded Q of the two modes adjusted to the same value, the structure becomes a symmetrical hybrid.

The normal modes of the generalized junction (i.e., when the diameters of the two shorting posts are different from each other) filled with ferrimagnetic material can be analyzed using the same approach taken by the author in a previous paper.[1]

Using cylindrical coordinates, where the Z axis and magnetic field lie in the symmetry axis of the junction, the characteristic equation can be derived. When the diameters of the two shorting posts become the same, the equation can be simplified to the following:

$$\frac{Y_n(x)}{J_n(x)} = \frac{Y_n'(y) \pm \frac{n}{y}\frac{K}{\mu} Y_n(y)}{J_n'(y) \pm \frac{n}{y}\frac{K}{\mu} J_n(y)} \tag{2}$$

and

$$\frac{Y_n(x)}{J_n(x)} = \frac{Y_n(y)}{J_n(y)} \tag{3}$$

where

$x = kr_1$

$y = kR$

$K = \omega \sqrt{\epsilon_0 \mu_0 \epsilon \mu_{eff}}$

r_1 = radius of the shorting post

R = normalized radius of the center conductor junction

K, μ = tensor permeability elements

$$\mu_{eff} = \frac{\mu^2 - K^2}{\mu}$$

Equation (2) determines the resonance frequency of the $TM_{n\ell 0}$ even modes, whereas, equation (3) that of the $TM_{n\ell 0}$ odd modes. The designation odd refers to those modes whose field have the same polarity on either side of the center conductor. The $TM_{n\ell 0}$ odd modes do not split in this case, the junction being completely filled with ferrimagnetic material. To solve for the frequency of the n = 0 mode and for the approximate center frequencies of the split modes, equation (2) can be simplified to the following:

$$\frac{Y_n(x)}{J_n(x)} = \frac{Y_n'(y)}{J_n'(y)} \tag{4}$$

The mode spectrum of the lowest few modes calculated from equations (3) and (4) is shown in Figure 2. According to equation (2) the $TM_{n\ell 0}$ modes split into "+" and "−" modes. Because of the splitting, several modes become degenerate to each other. The lowest degenerate modes of this type are the TM_{010} and the $TM_{\bar{1}10}$ modes. An experimental result demonstrating this degeneracy is shown in Figure 3.

In order to discuss the hybrid action, the $TM_{\bar{1}10}$ mode and the TM_{010} mode are examined separately. The $TM_{\bar{1}10}$ mode has an $e^{-i\Phi}$ component, and thus, the field rotates counter-clockwise at the same angular rate as the resonance frequency. This rotation is illustrated in Figure 4. Ports 3 and 4 which are located at $\Phi = -90°$ and $+90°$, sees the field which is excited at port 1, $\Phi = 0°$, T/4 behind and ahead respectively, while port 4 at $\Phi = 180°$ sees the excited field T/2 out of phase. On the other hand the TM_{010} mode does not have the $e^{i\Phi}$ component, and thus, the field has the same phase at each port.

With this relation established and, if the excited amplitudes of the modes are of the same value, the combination of the modes at ports 2, 3 and 4 result as illustrated in Figure 5. Namely, at port 2 the fields cancel and there is no output, and at ports 3 and 4, the outputs are −3dB and 90° out of phase from each other.

An experimental result obtained from the structure of Figure 1 is shown in Figure 6. The input match from 1.43 GHz to 1.57 GHz was within 1.20 VSWR. The balance of the two outputs was adjusted with a proper combination of the shorting post diameter, $4\pi M_0$ and thickness of the ferrite rings.

In order to have broadband performance it is necessary to stop the energy from entering the TM^{+}_{110} mode. This implies an increase in the splitting of the TM_{110} mode. One can accomplish this by proper choice of junction dimensions and ferrite parameters.

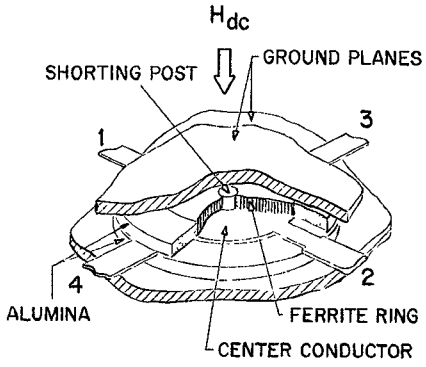

FIG. 1 - Assembly of Hybrid Structure

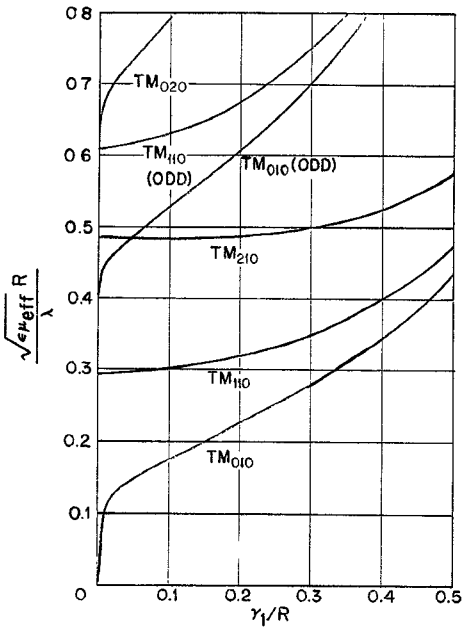

FIG. 2 - Junction Mode Spectrum

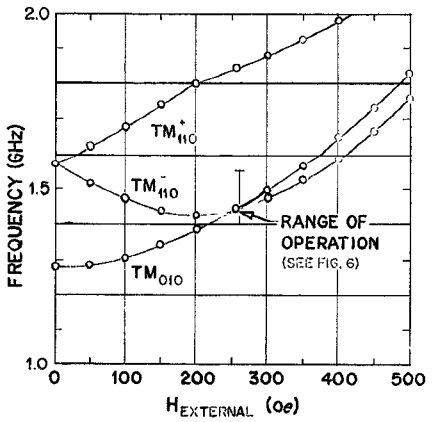

FIG. 3 - Two Lowest Modes as a Function $H_{external}$

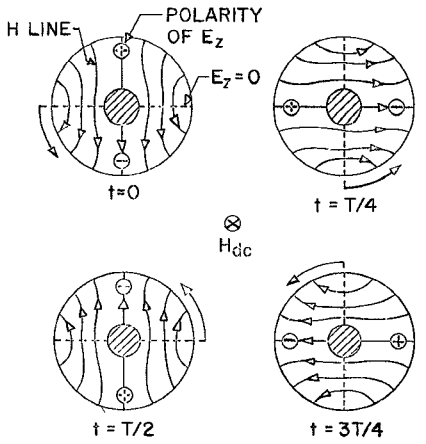

FIG. 4 - Time Variation of the TM_{110} Mode

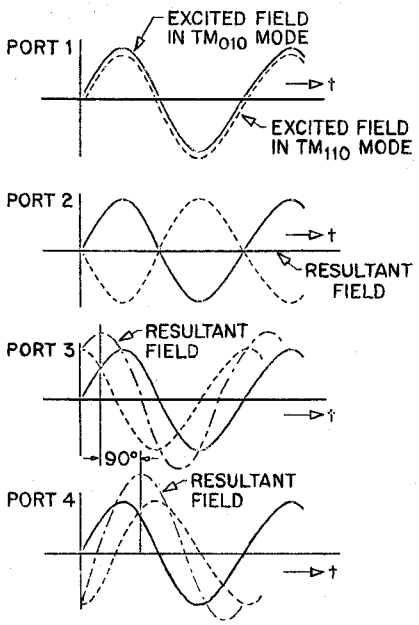

FIG. 5 - Resultant Fields at the Various Ports

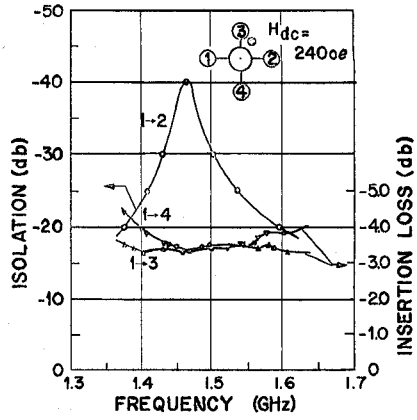

FIG. 6 - Measured Hybrid Performance